Collapse of the waiting time effect in a spin glass

Daniel M. Tennant [1,*] and Raymond L. Orbach[2]
[1]*Institute for Quantum Computing, University of Waterloo, Waterloo, Canada N2L 3G1*
[2]*Texas Materials Institute, The University of Texas at Austin, Austin, Texas 78712, USA*

(Received 11 May 2019; revised manuscript received 8 March 2020; accepted 14 April 2020; published 6 May 2020)

Waiting time measurements are reported for a bulk polycrystalline sample of the spin glass $Cu_{0.95}Mn_{0.05}$. We observe a suppression of aging as the glass temperature is approached from below. These results are interpreted in terms of a spin-glass correlation length approaching and reaching crystallite sizes. They provide a direct experimental connection between the correlation length scale and relaxation times in the spin-glass state. In particular, these measurements track the value of the dynamic critical exponent as the system transitions from the critical temperature regime to its low-temperature, quasistatic nonequilibrium phase.

DOI: 10.1103/PhysRevB.101.174409

I. INTRODUCTION

Aging is ubiquitous in complex systems [1]. Characterized by a large number of quasidegenerate ground states, they undergo an aging process where the system explores configuration space through a series of thermally induced jumps over a broad range of activation energies. This behavior was first observed in experiments on polymers by Struik [2] and is now recognized to be universal behavior for a large class of disparate physical systems such as glasses, spin glasses [3], and colloids [4].

Evidence for the existence of correlated domains has long been sought in glass-like systems [5]. This proposition has been validated by simulations of these systems, both in glasses [6–8] and spin glasses [9–13]. Experimental demonstrations of spatial correlations in real materials, however, has been difficult. In these materials, the two-point correlation function is indistinguishable between the high-temperature disordered state and the low temperature ordered phase. Therefore, domains of correlated regions are invisible to Bragg-type scattering experiments [14]. Nonetheless, many creative experiments have been carried out for both glasses [15,16] and spin glasses [17,18] that appear to confirm the presence of correlated regions in these disordered systems.

Measurements of correlated regions in spin glasses typically fall into two different temperature regimes. In the critical regime around the glass temperature, ac and dc measurements of the nonlinear magnetic susceptibility have been performed. In this temperature region, the system resides in thermal equilibrium. Hence, the scaling relationships between critical exponents hold and can be employed to deduce the size of correlated regions [19–22]. In the low-temperature, nonequilibrium phase, these relationships no longer hold, and alternative methods and analysis need to be developed. In particular, aging behavior, in the low-temperature nonequilibrium phase, has been shown to be correlated to the growth of domains [17,23].

From these experiments and others [18,24], along with simulations of these systems in the low-temperature regime [9,11,13], a consistent picture of the growth of domains in the low-temperature nonequilibrium phase has begun to emerge [25]. Results from these investigations indicate that correlations in $Cu_{1-x}Mn_x$ grow as a power law in time t,

$$\xi(t,T) = c_1 a_0 \left(\frac{t}{\tau_0}\right)^{c_2(T/T_g)}, \tag{1}$$

where c_1 and c_2 are empirically derived constants, a_0 is an average spatial separation between the magnetic species comprising the spin glass, T_g is the bulk spin-glass transition temperature, and τ_0 is the exchange time roughly equal to $\hbar/k_B T_g$. This form of the domain growth is consistent with the replica symmetry-breaking paradigm [26].

The three-dimensional spin glass is strongly believed to undergo a finite-temperature phase transition [22,27]. Therefore, at criticality, $T \sim T_g$, the exponent in Eq. (1), $c_2 \frac{T}{T_g}$ is equal to the inverse of the dynamic critical exponent, $1/z_c$. Multiple simulations of three-dimensional (3-D) Ising spin-glass models find a value of $1/z_c \sim 0.146$–0.149 [11–13] at criticality, in close agreement with our measurements here in the same temperature range. Our results extend measurements of c_2 from dynamics dictated from the finite-temperature critical point into the nonequilibrium phase. Our results qualitatively agree with previous simulations of 3-D Ising spin glasses [11,13] and also give context to previous discrepancies in reported values.

The measurements reported here depend on the ability to impose a mesoscopic length scale which halts the growth of spin-glass correlations on laboratory timescales. Previous measurements in this vein, deep in the low-temperature regime, have relied on high-quality thin-film samples to achieve this [18]. To probe the growth of correlations closer to the glass temperature, larger length scales are necessary, which polycrystalline samples can provide.

*dmtennant@uwaterloo.ca

 ©2020 American Physical Society

In three-dimensional polycrystalline materials, the borders between crystallites introduce additional nonmagnetic scattering of the Fermi-level conduction electrons. This results in the Ruderman–Kittel−Kasuya−Yosida interaction, responsible for mediating the exchange between magnetic impurities in a metallic spin glass, to become damped instead of oscillatory across a crystallite boundary [28]. The origin of spin-glass dynamics is thereby interrupted, leading to a cutoff of spin-glass correlations at roughly the crystallite size.

This work shows how aging in a bulk system becomes suppressed as the bulk transition temperature is approached. The results are interpreted through the growth of the correlation length to a length scale characteristic of crystallite size. As the critical temperature is approached, this takes place on shorter timescales, in accordance with Eq. (1). The results, within the restricted temperature range $0.89T_g$–$0.96T_g$, are consistent with a single value of c_2 but can also be interpreted as a temperature-dependent c_2 as the system transitions from its critical regime to its nonequilibrium phase.

II. PROCEDURE AND RESULTS

The bulk $Cu_{0.95}Mn_{0.05}$ sample, $T_g = 27.5$ K, was prepared by alloying 99.995% Cu and 99.95% Mn. The sample was then annealed at 900 °C for 24 hours, followed by a rapid thermal quench to 77 K. This process results in a bulk comprised of mesoscopic crystallites. By employing Debye-Scherrer analysis on the width of the x-ray Bragg peak, as well as scanning electron microscopy, it was determined that more than 90% of crystallites have a diameter within 10 nm of 80 nm [23]. At this concentration, the average Mn-Mn spatial separation is $a_0 \approx 0.691$ nm. The exchange rate, $1/\tau_0 \approx k_B T_g/\hbar$ is approximately 3.6×10^{12} Hz.

The experimental protocol for the thermoremanent magnetization (TRM) measurement begins with preparing the sample above T_g in a small magnetic field, typically 20 G. A fast cooling protocol was employed, generally reaching a stable measuring temperature, T_m, within 30–50 seconds of the temperature quench. Upon stabilizing at the T_m, the sample was held there, with the field on, for various waiting times, after which the field is cut to zero and the TRM is observed for 1–4 $\times 10^4$ s depending on the waiting time t_w. After a prescribed measurement time t_m, the temperature is raised above T_g, then lowered back to T_m, and the concomitant magnetization is subtracted from the data set, effectively removing everything but the spin-glass signal from our data.

The TRM measurements were taken on a custom built magnetometer housed at Indiana University of Pennsylvania (IUP). The IUP magnetometer exhibits a resolution of ±11 nano-e.m.u. as well as a stable temperature to within 0.6 mK over the course of 12 hours, the typical timescale of an experimental run. Recent improvements to the machine ensure a barometric stability within 0.1 torr over the same timescales. The pressure stability ensures that low-frequency drifts do not corrupt our signal, allowing us to trust the validity of our signal over the entire course of the measurement time.

In this work, aging in spin glasses is characterized by the structure of the logarithmic time derivative of the magnetization through the quantity $S(t) = -dM(t)/d\ell nt$ for the TRM measurements. The $S(t)$ curve is related to the Laplace transform of the TRM in that they both share the same peak and hence carry information on the distribution of spin-glass relaxation times.

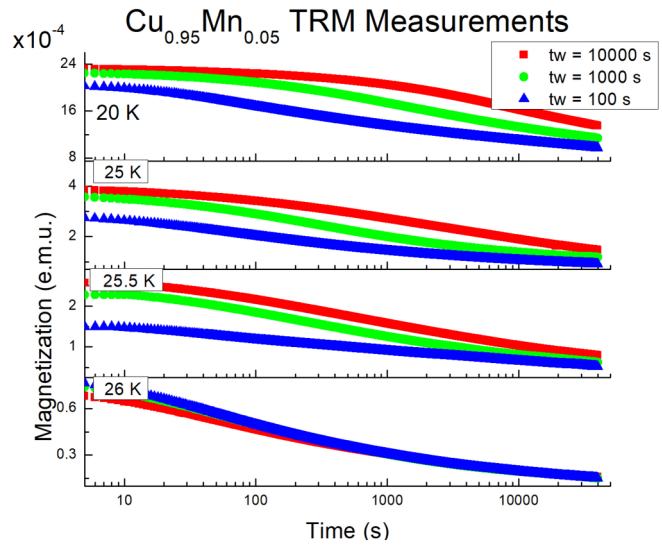

FIG. 1. Thermoremanent magnetization measurements, made in 20 G, for a range of temperatures. For lower temperatures, the effect of the waiting time is most apparent. As the glass temperature is approached, the effect of the waiting time becomes less pronounced.

Figure 1 exhibits the raw data for the time decay of the TRM at various quench temperatures. Figure 2 takes the data from Fig. 1 and creates the $S(t) = -dTRM/d\ell nt$ curves. Results show the waiting time effect, as quantified by the peak of the $S(t)$ curve, gradually collapsing in the temperature range $0.89T_g$–$0.96T_g$.

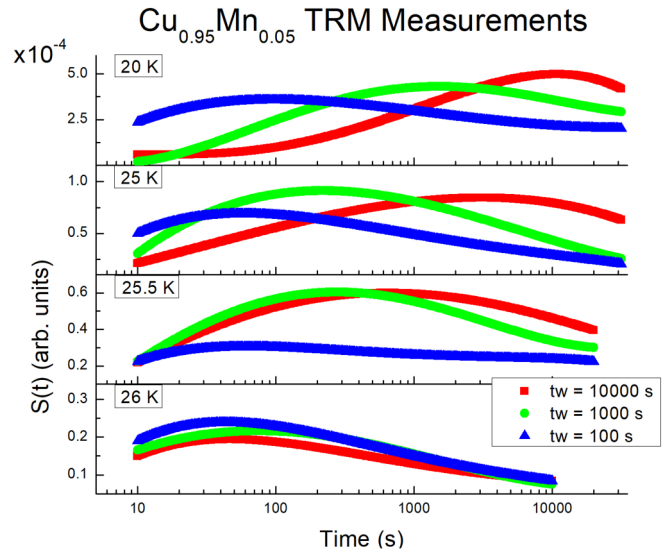

FIG. 2. The corresponding $S(t)$ curves for the TRM measurements in Fig. 1. At the lower temperature, 20 K, the peak of the $S(t)$ curves reflect the waiting time of the measurement. As the glass temperature is approached, the $S(t)$ peaks occur at shorter timescales until the waiting time has no discernible effect.

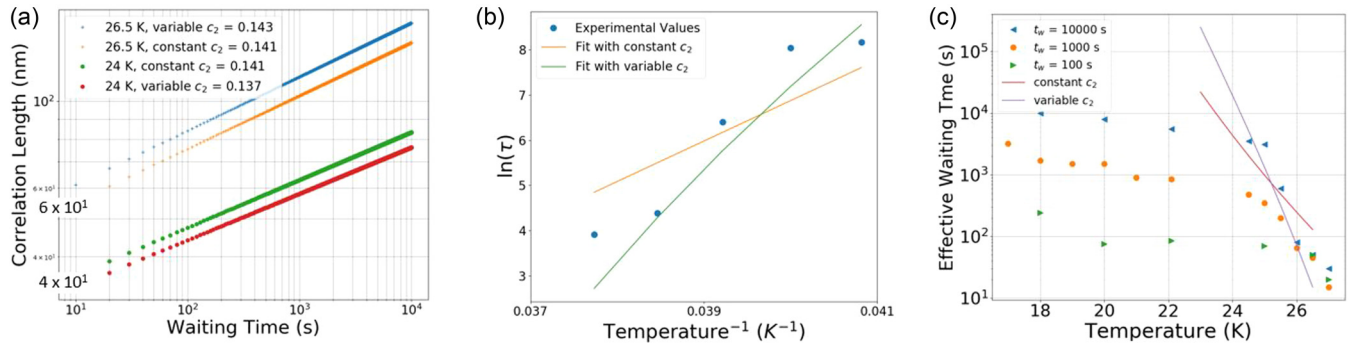

FIG. 3. (a) The spin-glass correlation growth as described by Eq. (1) is shown for 24 and 26.5 K for both a constant value of $c_2 = 0.141$ as well as the variable value, $c_2 = 0.134$–0.150. For both cases, the correlation length reaches 80 ± 10 nm in 100 s for the 26.5 K case and in 10^4 s for the 24 K case. (b) The relaxation times as a function of inverse temperature. Shown are the fits assuming both a constant c_2 value and also a variable value. Both fits use the previously stated value of τ_o. The variable c_2 fit provides a closer approximation to the measurements. (c) Shown are the measured values of the relaxation times as determined by the peaks of $S(t)$. Also displayed are the relaxation times predicted by both the constant and variable c_2 models. Note how the measured and predicted values of the relaxation time diverge for $T < 24$ K, indicating the analysis in terms of spin-glass correlations reaching the crystallite size during the 10^4 s waiting time no longer applies.

III. DISCUSSION

Previous analysis of TRM decays in spin glasses have also displayed anomalies in the same temperature range as those probed in this set of experiments. Earlier studies of the waiting time effect were expressed in terms of scaling the TRM decays. It was shown that TRM decays at various waiting times would superpose if the measuring time was scaled as λ/t_w^{μ} [29,30]. For temperatures less than $0.90T_g$, $\mu \approx 0.9$. However, for temperatures greater than $0.90T_g$, the value of μ steadily dropped to maintain superposition. Our results are consistent with this analysis: the magnitude of the waiting time progressively has less of an effect on the time dependence of the TRM as the temperature is increased above $0.89T_g$. Our work provides some insight as to why scaling exhibits this anomaly over the temperature range $T/T_g > 0.89$.

Our results can be interpreted as the size of spin-glass correlations becoming comparable to the size of the mesoscopic crystallites comprising our macroscopic sample. At this point the growth of $\xi(t, T)$ is halted, and for a relatively narrow range of crystallite sizes, the TRM decay will be dominated by a single activation energy, which, through the Arrhenius law, $\tau(T) = \tau_o e^{\Delta/k_b T}$, can be related to a temperature-dependent relaxation time. By combining the Arrhenius relation with Eq. (1), it is straightforward to show that the activation energy has a logarithmic dependence on the length scale of the spin-glass correlations, in our case the typical crystallite size $\mathcal{L}$:

$$\frac{\Delta(t,T)}{k_B T_g} = \frac{1}{c_2}\left[\ell n\left(\frac{\mathcal{L}}{a_0}\right) - \ell n c_1\right]. \tag{2}$$

To illustrate this point, consider a TRM decay in the temperature range $T_m > 0.89T_g$ such that the spin-glass correlations reach the crystallite size within the waiting time of the measurement. The subsequent TRM is then dominated by a relaxation time defined by the length-dependent activation energy and the measurement temperature. The TRM then has the relatively simple form

$$M_{\mathrm{TRM}}(t) = m_o e^{-t/\tau(T)}, \tag{3}$$

and the resultant $S(t)$ curve is found to be

$$S(t) \sim \frac{t}{\tau} e^{-t/\tau}. \tag{4}$$

The peak of this function occurs at the activation-energy-dependant τ, as defined through the Arrhenius relationship.

To extract values of c_2 over the range of temperatures measured, it is necessary to simultaneously fit the growth of correlations, described by Eq. (1), to the relevant temperature range as well as to the relaxation times, extracted from the $S(t)$ curves in that temperature range. The $S(t)$ curves start to collapse onto one another around 24 K, or $0.89T_g$. We take this as evidence that the spin-glass correlations have just reached the crystallite boundaries for the longest waiting time, $t_w = 10^4$ s. Likewise, the $S(t)$ curves have completely collapsed onto one another at $T = 26.5$ K, or $0.96T_g$ indicating that the spin-glass correlations have reached the crystallite boundaries even for the shortest waiting time $t_w = 100$ s.

Values of c_1 and c_2 that return 80 ± 10 nm in Eq. (1) for $t_w = 10^4$ s at 24 K and $t_w = 100$ s at 26.5 K, as displayed in Fig. 3(a), were found to be $c_1 = 1.15 \pm 0.05$, $c_2 = 0.141 \pm 0.004$, and $\Delta = 899 \pm 17$ K. The uncertainties are based on the uncertainties of the length scale. The full test of the consistency of our analysis is fitting the relaxation times in this temperature region, as determined by the peaks of the $S(t)$ curves, to the Arrhenius law to extract the activation energy. The fit is performed solely on the $t_w = 10^4$ s data points, ensuring that the spin-glass correlations have reached the crystallite boundaries within the waiting time. As shown in Fig. 3(b), fitting the relaxation times in the relevant temperature range returns a value for the activation energy of $\Delta = 895 \pm 11$ K, which agrees with the value of Δ determined by the correlation-length growth.

While these measurements, in this restricted temperature range, are consistent with constant values of c_2 and Δ, they can also be interpreted in the context of temperature-dependent values. Recent numerical work on Ising spin glasses show the value of c_2 to change as the system transitions from critical dynamics in the immediate vicinity of the glass temperature to nonequilibrium dynamics in the

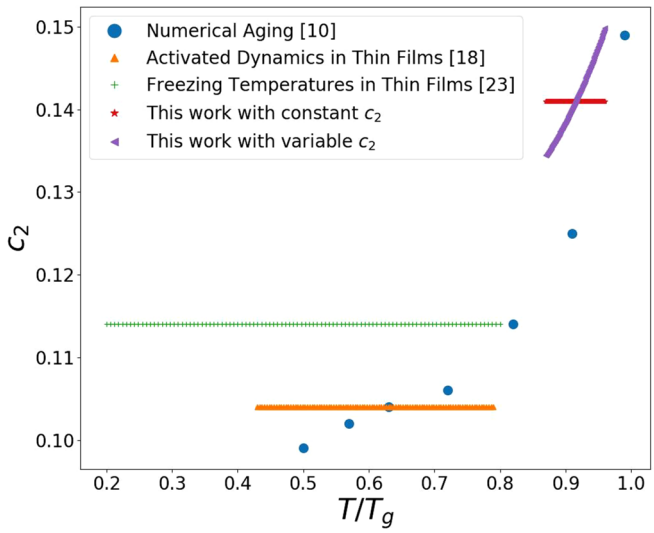

FIG. 4. Reported values for c_2 resulting from both experimental and numerical studies. All reported experimental data are taken from $Cu_{1-x}Mn_x$ samples while the numerical work is taken solely from three-dimensional Ising spin glasses with $\pm J$ coupling [37]. Both the constant and variable c_2 analysis is presented, clearly showing the transition between critical dynamics and the nonequilibrium phase.

low-temperature phase [11,13]. A useful metric, the ratio of the Josephson length [31], $l_J \propto (T_c - T)^{-\nu}$, to the spin-glass correlation length,

$$x(t_w, T) = l_J(T)/\xi(t_w, T), \tag{5}$$

has recently been used to quantify this transition [32]. For $x \gg 1$, where the Josephson length dominates, we expect critical behavior, while for $x \ll 1$, we expect the nonequilibrium growth of correlated domains to be the main influence on the dynamics of the system. For a fixed length of 80 nm, and the metallic spin-glass critical length exponent, $\nu = 1.3$ [21,33], we find this transition at a temperature of 26.8 K, right at the upper range of our measurements. Hence, our measurements probe the spin-glass dynamics precisely as the system is transitioning out of critical behavior.

Considering a temperature dependence of c_2 inspired by Ref. [13], fits to the correlation length growth in the relevant temperature region and experimental waiting times can be performed. As shown in Fig. 3(a), the correlation length reaches the polycrystalline length scale for the expected waiting times and temperatures. For the temperature range $0.89T_g$–$0.96T_g$, the values for c_2, as shown in Fig. 4, span 0.134–0.150. Comparing the values of the relaxation times, as predicted by the variable c_2, with the fit of the relaxation times while considering a constant c_2, actually show the variable c_2 predictions more closely follow the measured relaxation times.

IV. SUMMARY AND CONCLUSIONS

The measurements reported here represent the first determination of the growth of correlations as the system transitions from the finite-temperature critical regime to its low-temperature, nonequilibrium phase. The low-temperature measurements [18,24], as well as simulation in that temperature region are entirely consistent with a constant value of $c_2 = 0.107 \pm 0.007$. Experimental [23] as well as numerical work [11–13] in the critical regime report a value of $c_2 = 0.147 \pm 0.003$. This value is slightly lower than the critical dynamic exponent $1/z_c = 0.161$–0.167 reported in Refs. [22,34–36]. The larger values were found by ensuring that the system was in thermal equilibrium both in simulation and experimental work. Figure 4 illustrates the temperature dependence of c_2 over a range of experiments and simulation work.

Nonequilibrium behavior, such as aging, is typically seen as a hindrance to observing the true, equilibrium properties of the system. This work *exploits* nonequilibrium phenomena to measure correlated length scales [38]. Aging, in samples at the mesoscale, enables us to ascertain the relationship between length scales and relaxation times in an ordered but not equilibrated state. Our findings are entirely consistent with the power-law dynamics predicted through Eq. (1). In addition, they provide experimental evidence for the transition from dynamics controlled by the $T = 0$ fixed point for temperatures well below T_g, to the critical region close to the glass temperature.

ACKNOWLEDGMENTS

This work was supported by the U.S. Department of Energy, Office of Basic Energy Sciences, Division of Materials Science and Engineering, under Award No. DESC0013599 and Contract No. DE-AC02-07CH11358.

[1] J. P. Bouchaud, *Aging in Glassy Systems: New Experiments, Simple Models, and Open Questions* (Service de Physique de l'Etat Condensé, CEA Saclay, Gif sur Yvette, 2008).

[2] L. C. E. Struik, *Physical Aging in Amorphous Polymers and Other Materials* (Elsevier, Houston, 1978).

[3] E. Vincent, J. Hammann, M. Ocio, J.-P. Bouchaud, and L. F. Cugliandolo, Slow dynamics and aging in spin glasses, in *Complex Behaviour of Glassy Systems, Proceedings of the XIV Sitges Conference*, Lecture Notes in Physics, edited by M. Rubi and C. Perez-Vicente (Springer, Berlin, 1996), Vol. 492.

[4] L. Cipelletti, S. Manley, R. C. Ball, and D. A. Weitz, Phys. Rev. Lett. **84**, 2275 (2000).

[5] G. Adam and J. Gibbs, J. Chem. Phys. **43**, 139 (1965).

[6] G. Biroli, J.-P. Bouchaud, A. Cavagna, T. S. Grigera, and P. Verrocchio, Nat. Phys. **4**, 771 (2008).

[7] R. Pinney, T. B. Liverpool, and C. P. Royall, J. Chem. Phys. **143**, 244507 (2015).

[8] L. Berthier, P. Charbonneau, and S. Yaida, J. Chem. Phys. **144**, 024501 (2016).

[9] H. Rieger, J. Phys. A: Math. Gen. **26**, L615 (1993); H. Rieger, B. Steckemetz, and M. Schreckenberg, Europhys. Lett. **27**, 485 (1994).

[10] T. Komori, H. Yoshino, and H. Takayama, J. Phys. Soc. Jpn. **68**, 3387 (1999).

[11] F. Belletti, M. Cotallo, A. Cruz, L. A. Fernandez, A. Gordillo-Guerrero, M. Guidetti, A. Maiorano, F. Mantovani, E. Marinari, V. Martin-Mayor *et al.* Phys. Rev. Lett. **101**, 157201 (2008).
[12] M. Lulli, G. Parisi, and A. Pelissetto, Phys. Rev. E **93**, 032126 (2016).
[13] M. Baity-Jesi, E. Calore, A. Cruz, L. A. Fernandez, J. M. Gil-Narvion, A. Gordillo-Guerrero, D. Iñiguez, A. Maiorano, E. Marinari, V. Martin-Mayor *et al.*, Phys. Rev. Lett. **120**, 267203 (2018).
[14] S. A. Werner, J. J. Rhyne, and J. A. Gotass, Solid State Commun. **56**, 457 (1985).
[15] L. Berthier, G. Biroli, J.-P. Bouchaud, L. Cipelletti, D. El Masri, and D. L'Hôte, Science **310**, 1797 (2005).
[16] S. Albert, Th. Bauer, M. Michl, G. Biroli, J.-P. Bouchaud, A. Loidl, P. Lunkenheimer, R. Tourbot, C. Wiertel-Gasquet, and F. Ladieu, Science **352**, 1308 (2016).
[17] Y. G. Joh, R. Orbach, G. G. Wood, J. Hammann, and E. Vincent, Phys. Rev. Lett. **82**, 438 (1999).
[18] Q. Zhai, D. C. Harrison, D. Tennant, E. D. Dalhberg, G. G. Kenning, and R. L. Orbach, Phys. Rev. B **95**, 054304 (2017).
[19] H. Bouchiat, J. Phys. (Paris) **47**, 71 (1986).
[20] Ph. Refregier, E. Vincent, M. Ocio, and J. Hammann, Jpn. J. Appl. Phys. (1962–1981) **26**, 783 (1987).
[21] L. P. Levy, Phys. Rev. B **38**, 4963 (1988).
[22] K. Gunnarsson, P. Svedlindh, P. Nordblad, L. Lundgren, H. Aruga, and A. Ito, Phys. Rev. B **43**, 8199 (1991).
[23] G. G. Kenning, D. M. Tennant, C. M. Rost, F. G. da Silva, B. J. Walters, Q. Zhai, D. C. Harrison, E. D. Dahlberg, and R. L. Orbach, Phys. Rev. B **98**, 104436 (2018).
[24] G. G. Kenning, J. Bass, W. P. Pratt, D. Leslie-Pelecky, L. Hoines, W. Leach, M. L. Wilson, R. Stubi, and J. A. Cowen, Phys. Rev. B **42**, 2393 (1990).
[25] S. Guchhait, G. G. Kenning, R. L. Orbach, and G. F. Rodriguez, Phys. Rev. B **91**, 014434 (2015).
[26] E. Marinari, G. Parisi, F. Ricci-Tersenghi, J. J. Ruiz-Lorenzo, and F. Zuliani, J. Stat. Phys. **98**, 973 (2000).
[27] M. Baity-Jesi, R. A. Banos, A. Cruz, L. A. Fernandez, J. M. Gil-Narvion, A. Gordillo-Guerrero, D. Iniguez, A. Maiorano, F. Mantovani, E. Marinari *et al.*, Phys. Rev. B **88**, 224416 (2013).
[28] T. Kasuya, *s-d* and *s-f* interaction and rare earth metals, in *Magnetism*, Vol. IIB, edited by G. T. Rado and H. Suhl (Academic, New York, 1966), pp. 215–294.
[29] M. Alba, M. Ocio, and J. Hammann, Europhys. Lett. **2**, 45 (1986).
[30] M. Alba, J. Hammann, M. Ocio, Ph. Refregier, and H. Bouchait, J. Appl. Phys. **61**, 3683 (1987).
[31] B. D. Josephson, Phys. Lett. **21**, 608 (1966).
[32] Q. Zhai, V. Martin-Mayor, D. L. Schlagel, G. G. Kenning, and R. L. Orbach, Phys. Rev. B **100**, 094202 (2019).
[33] N. de Courtenay, H. Bouchait, H. Hurdquint, and A. Fert, J. Phys. (Paris) **47**, 1507 (1986).
[34] A. T. Ogielski, Phys. Rev. B **32**, 7384 (1985).
[35] L. W. Bernardi, S. Prakash, and I. A. Campbell, Phys. Rev. Lett. **77**, 2798 (1996).
[36] T. Nakamura, S. Endoh, and T. Yamamoto, J. Phys. A: Math. Gen. **36**, 10895 (2003).
[37] While it is debatable how exactly this model describes $Cu_{1-x}Mn_x$, there is strong qualitative agreement between the two systems. Also, both systems represent the most studied examples of material and simulated spin glasses and are the only systems studied in the full temperature range presented.
[38] G. Biroli and J. P. Garrahan, J. Chem. Phys. **138**, 12A301 (2013).